Recombinant Irisin

Subjects: Medicine, Research & Experimental

Contributor: Maria Grano

Irisin promotes bone formation in the bony callus and accelerates the fracture repair process, suggesting a possible use as a novel pharmacologic modulator of fracture healing.

irisin fracture bone muscle chondrocytes

1. Introduction

Bone fractures have a high incidence in the world population and are often associated with significant disability, imposing high social and health care costs [1]. In 2010, it was estimated that the number of individuals aged >50 years at high risk for osteoporotic fracture worldwide was 158 million, which is expected to double by 2040. The economic burden of fractures has been estimated at 37 billion, with the costs expected to increase by 25% by 2025 [2].

In many cases, fractures heal devoid of adverse outcomes. However, delayed healing may occur in some patients, particularly in those suffering metabolic or vascular disorders. In such cases, surgery is necessary to increase stability and/or promote healing [3][4]. The development of pharmacological agents could provide alternative or additional new approaches to accelerate fracture healing [5].

Fracture healing is a multiphasic process that generally requires months to be completed [6]. Immediately after the initial inflammatory and hematoma phases, the recruitment of mesenchymal progenitor cells leads to the formation of a fibrocartilaginous or soft callus, which is crucial for early stability of the fracture site [7]. As healing progresses, formation of the cartilage callus occurs, and chondroblasts, typically expressing collagen Type II (COL II) matrix protein and transcription factor SRY (sex determining region Y)-box 9 (SOX9), gradually undergo differentiation, lose the expression of the above markers and acquire those typical of hypertrophic chondrocytes, such as collagen Type X (COL X) [8].

The cartilaginous callus turns into the bony callus due to the replacement of cartilage by bone through a process reminiscent of the events occurring during endochondral bone development including the crucial bone-forming activity of osteoblasts, which express the runt related transcription factor 2 (RUNX2). An essential role is also played by osteoclasts, which resorb the cartilage callus and cooperate with osteoblasts for the proper remodeling of the bony callus [9].

Numerous studies, mostly in animal models, have investigated the effect of some bone anabolic agents, such as BMPs, FGFs, activators of the Wnt/Î²catenin pathway and PTH/PTHrP receptor agonists [10], in accelerating fracture repair.

Although left unexplored, previous observations have suggested that fracture healing is more efficient when there are muscle flaps present in the area of injury [11]. This pioneering observation was recently brought to light by recent evidence showing that skeletal muscle is an endocrine organ that produces hormone-like molecules, called myokines, with an endocrine/paracrine action on bone tissue [12]. The hormone-like myokine irisin is a newly discovered molecule affecting bone metabolism and it has never been studied as a treatment for fracture healing before.

Irisin, produced by skeletal muscle during exercise, was initially described as crucial for inducing the browning of white adipose tissue, but shortly thereafter, pleiotropic effects emerged in several tissues and organs (bone, muscle, cartilage, pancreas, liver and brain) [13][14]. Previous studies were the first to prove that the musculoskeletal system is likely to be an important target, as an irisin dose 35 times lower than that effective on adipose tissue, increased bone mass in healthy mice [15], and prevented bone and muscle losses in an osteo-sarcopenic mouse model of disuse-induced osteoporosis and muscle atrophy [16].

These studies showed that irisin treatment in vitro enhanced osteoblast differentiation [17] and improved bone mass in young adult mice in vivo by raising the tibial diaphyseal cross-sectional area due to an enhanced osteoblast activity and bone formation [15]. It was also shown that 100 ng/mL of recombinant irisin directly acts on osteoblasts [17] and osteocytes [18] by activating Erk1/2 phosphorylation and increasing the expression of the Activating Transcription Factor 4 (Atf4), a key transcription factor for osteoblast proliferation, differentiation and survival [15]. In contrast with these results, Kim and colleagues showed that mice with global deletion of the irisin precursor, the Fibronectin Type III Domain Containing 5 (FNDC5), were resistant to ovariectomy-induced bone loss through inhibition of osteoclastic bone resorption and osteocytic osteolysis [19]. In vitro data showed that continuous exogenous treatment with 10 ng/mL irisin stimulated osteoclast differentiation from bone marrow precursors. However, increasing the dose to 20 ng/mL had a lower effect on osteoclast number, and doses of irisin equal or exceeding 100 ng/mL decreased osteoclastogenesis [20]. Therefore, it has been hypothesized that the opposing effects of irisin could be due to its concentration, as well as the duration or frequency of treatment. Since its discovery, some reports have questioned the existence of circulating irisin in humans, both because human FNDC5 has a non-canonical ATA translation start and because of the previous unreliable assay methods used for its detection [21]. In 2015, the study by Jedrychowski and colleagues demonstrated by tandem mass spectrometry that irisin is expressed in humans and is regulated by exercise through the detection and quantification of circulating human irisin at a concentration of ~4 ng/mL [22]. Conversely, another study also using mass spectrometry demonstrated that irisin was not present in human plasma but was detectable in cerebrospinal fluid samples in the range of 0.3 to 1.9 ng/mL [23]. Although quantification of irisin by mass spectrometry should be the gold standard for determining its concentration, this technique requires multi-step sample preparation, such as removal of albumin and immunoglobulins, which could lead to variable amounts of protein being retained for analysis and result in uncontrollable variations in the measurement of irisin [24]. However, since the discovery of irisin, numerous studies have proposed a role of irisin in multi-organ protection in humans, and much progress has also been made to demonstrate its key role as one of the determinants of skeletal status. Human studies have shown that postmenopausal women with previous osteoporotic fractures had low irisin levels [25] and that circulating irisin was inversely related to vertebral fragility fractures [26]. Furthermore, previous work demonstrated a positive association between circulating irisin levels and bone mineral status in adult and child populations [27][28][29][30]. More recently, it was reported that low concentrations of irisin in older women were associated with an increased risk of hip fractures [31].

Notably, the levels of the irisin precursor, FNDC5, in the skeletal muscle of the older adult subjects were positively associated with irisin serum levels and osteocalcin mRNA expression in bone biopsies, indicating a strong correlation between healthy muscle and bone tissues [29].

Moreover, recent findings highlighted that irisin also targets cartilage. An in vitro study of human osteoarthritic chondrocytes showed that the myokine directly affects chondrocytes and improves cellular anabolism while decreasing their catabolism [32]. Additionally, irisin signaling was required to protect against oxidative damage, apoptosis and extracellular matrix underproduction in inflamed chondrocytes, delaying osteoarthritis development [33].

2. Irisin Induces Maturation of the Soft Callus at 10 Days Post-Fracture

X-ray radiography performed directly after surgery confirmed transverse mid-diaphyseal tibial fractures and the adequate positioning of intramedullary pins (**Figure 1**A). Serial radiographs of representative mice, intermittently treated with normal saline (vehicle) or irisin, showed clearly visible fracture lines in both treatment groups at 10 days post-fracture (**Figure 1**B,C). To determine the total cartilage area within the soft callus, Safranin-O staining was performed at the same time point (**Figure 1**D). Histological analysis revealed increased callus area but lower proteoglycan content in the soft callus of irisin-treated mice (**Figure 1**D). The histological observation was confirmed by morphometric analysis of the entire callus, showing a significantly higher percentage of soft callus area (+25%; p = 0.0114) but lower proteoglycan content (â40%; p = 0.0018) in irisin-treated mice compared with control mice. Furthermore, tartrate-resistant acid phosphatase (Trap)-positive osteoclasts within the callus tissue were also assessed by histology (**Figure 1**G). Quantification of Trap-positive (Trap+) cells within the callus area showed a 2.4-fold increase in osteoclast numbers on the callus area (OC N. /CA) at 10 days (p = 0.026) after fracture in irisin-treated mice (**Figure 1**H), thus suggesting a different stage of soft callus formation following treatment with irisin. To decipher the factors involved in irisin-induced cartilaginous callus formation, we performed an immunohistochemical analysis of the matrix proteins and transcription factors expressed by the chondrocytes during their progression to the hypertrophic phenotype.

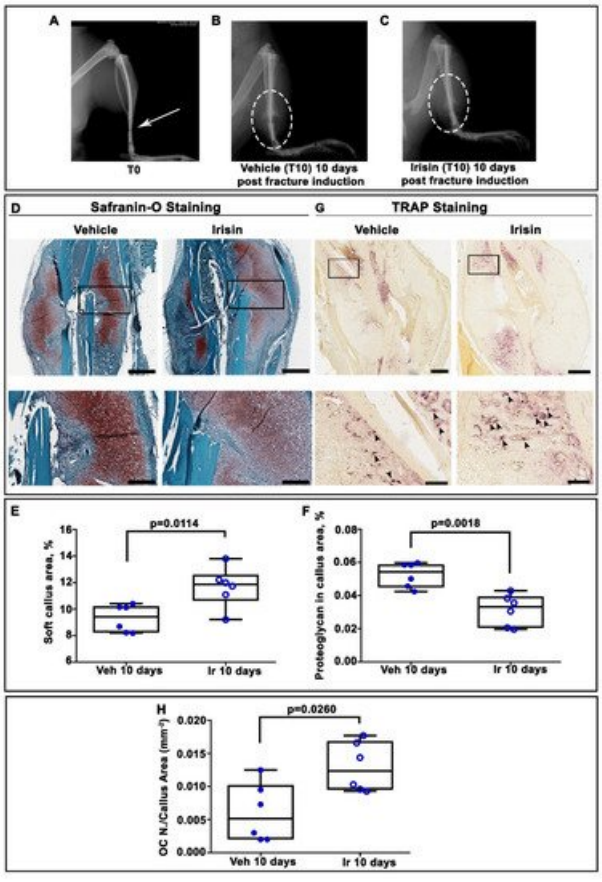

Figure 1. (**A**) Representative radiological images of fractured tibia at Time 0 (T0), and mice intermittently treated with (**B**) normal saline (vehicle) or (**C**) irisin at 10 days post-fracture. (**D**) Representative Safranin O-staining images of callus sections from vehicle- and irisin-treated mice at 10 days post-fracture (scale bar 0.8 mm). The black squares indicate the areas of higher magnification (scale bar: 60 Î¼m). (**E**) Dot-plot graphs showing the increased soft callus area and (**F**) decreased proteoglycan-rich cartilage matrix in irisin-treated mice (n = 6) compared with vehicle-treated mice (n = 6). (**G**) Representative Trap staining images of callus sections from vehicle- (n = 6) and irisin-treated (n = 6) mice at 10 days post-fracture (scale bar: 0.8 mm). The

black squares indicate the areas of higher magnification. (**H**) Dot-plot graph showing the significantly increased number of Trap-positive cells in the callus area (OC n. /CA) in irisin-treated mice (n = 6) compared with vehicle-treated mice (n = 6) (scale bar: 60 Î¼m). Data are presented as dot-plots with medians, from maximum to minimum, with all data points shown. The MannâWhitney test was used to compare groups.

Immunohistochemical staining for COL II in callus sections (**Figure 2**A) and relative quantification (**Figure 2**B) showed no significant difference between the two experimental groups. However, the expression of COL X, a well-established marker of hypertrophic chondrocytes, was increased threefold (p = 0.0012) in the callus of irisin-treated mice compared with the vehicle group (**Figure 2**C,D). Of note, the positivity for the master regulator of osteoblast differentiation, RUNX2, was 2.2-fold higher (p = 0.0137) (**Figure 2**E,F), whereas the positivity for SOX9, the transcription factor that regulates chondrogenesis, was twofold lower (p = 0.0058) (**Figure 2**G,H) in the callus of irisin-treated mice than in the vehicle-treated group.

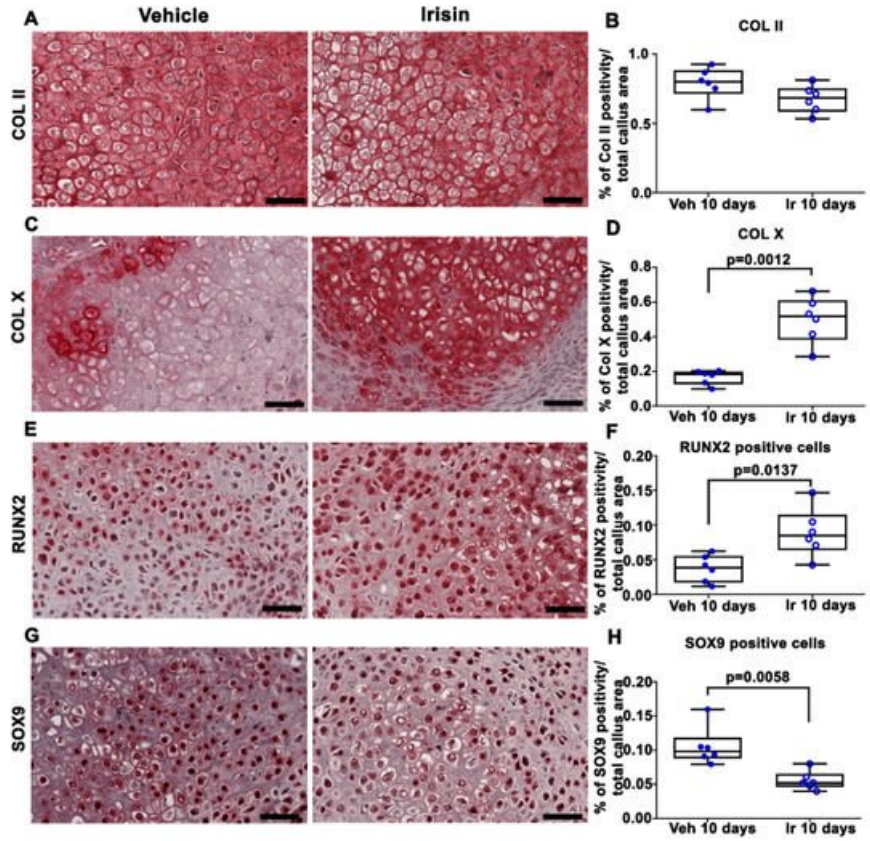

Figure 2. Representative images of (**A**) COL II, (**C**) Col X, (**E**) RUNX2 and (**G**) SOX9 immunostaining in callus sections from vehicle-treated mice (n = 6) and irisin-treated mice (n = 6) at 10 days post-fracture (scale bars: 20 Âμm). Dot-plot graphs showing the quantification of (**B**) COL II, (**D**) COL X, (**F**) RUNX2 and (**H**) SOX9 expression. Data are presented as dot-plots with medians, from maximum to minimum, with all data points shown. The MannâWhitney test was used to compare groups.

3. Irisin Increased Bony Callus Size at 28 Days Post-Fracture

After 28 days post-fracture, X-ray images showed that callus was still evident in both vehicle- and irisin-treated mice (**Figure 3**A). However, longitudinal and cross-sectional micro-computed tomography (microCT) 3D reconstructions (**Figure 3**B,C) clearly indicated an increased callus size in the tibia of irisin-treated mice. Due to the absence of mineralization of the callus at 10 days post-fracture, microCT analysis was performed only on the callus at 28 days post-fracture. Callus

total volume (Cal TV) (**Figure 3**D) and callus bone volume (Cal BV) (**Figure 3**E) increased by 68% ($p = 0.0003$) and 67% ($p = 0.00193$), respectively, in irisin-treated mice compared with the control group, resulting in an unchanged callus bone volume fraction (Cal. BV/TV) (**Figure 3**F). Moreover, the bone mineral content of the callus (Cal. BMC) (**Figure 3**G) was 74% higher ($p = 0.0012$) in irisin-treated mice than in the controls, whereas the callus bone mineral density (cal. BMD) (**Figure 3**H) was unchanged. Consistent with the unchanged bone volume fraction in the callus, measurements of trabecular parameters showed that there was no significant difference in trabecular thickness (Cal. Tb. Th) (**Figure 3**I), trabecular separation (Cal. Tb. Sp) (**Figure 3**J) and trabecular number (Cal. Tb. N) (**Figure 3**K) between the two groups of mice.

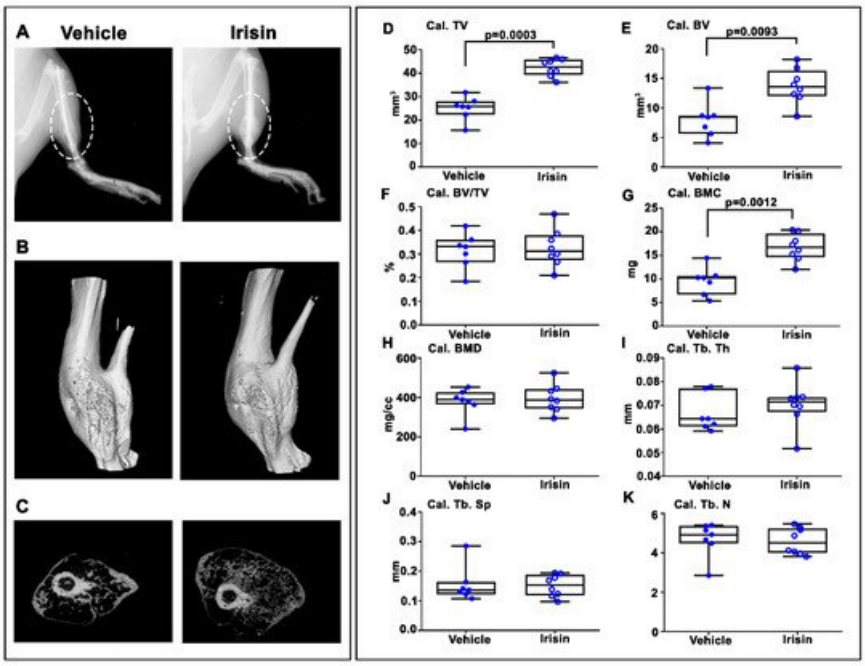

Figure 3. Mice sacrificed at 28 days post-fracture. (**A**) Representative radiological images. (**B**) Longitudinal and (**C**) cross-sectional micro-computed tomography (Î¼CT) 3D reconstructions of fractured tibiae from vehicle- and irisin-treated mice at 28 days post-fracture. ÂµCT analysis of the bone callus: (**D**) Cal. TV= callus total volume; (**E**) Cal. BV= callus bone volume; (**F**) Cal. BV/TV= callus bone volume/total volume; (**G**) Cal. BMC = callus bone mineral content; (**H**) Cal. BMD = callus bone mineral density; (**I**) Cal. Tb. Th = callus trabecular thickness; (**J**) Cal. Tb. Sp = callus trabecular separation; (**K**) Cal. Tb. n= callus trabecular number. Vehicle-treated mice (n = 7); irisin-treated mice (n = 8). Data are presented as box-and-whisker plots with median and interquartile ranges, from maximum to minimum, with all data points shown. The MannâWhitney test was used to compare groups.

4. Irisin Accelerated Bony Callus Formation at 28 Days Post-Fracture

To further characterize the influence of irisin treatment on the structural organization of the bony callus at 28 days post-fracture, we performed histological and immunohistochemical analysis of callus sections. Hematoxylin and eosin staining showed that irisin promoted the formation of bony callus (**Figure 4**A), thereby accelerating fracture healing. In contrast, in vehicle-injected mice, the fibrous tissue was still prevalent in the fracture gap. Trap staining (**Figure 4**B) of callus sections and the relative morphometric analysis (**Figure 4**D) showed the decreasing, although not significant, trend of the osteoclast number in the callus area (OC N./CA) in irisin-treated mice compared with the vehicle group. Interestingly, immunohistochemistry for osteocalcin (**Figure 4**C) revealed a higher percentage of positive cells for this bone matrix protein (+26%; $p = 0.0019$) (**Figure 4**E) in irisin-treated mice, thus suggesting that irisin promotes bone formation in the bony callus, possibly improving the fracture repair process.

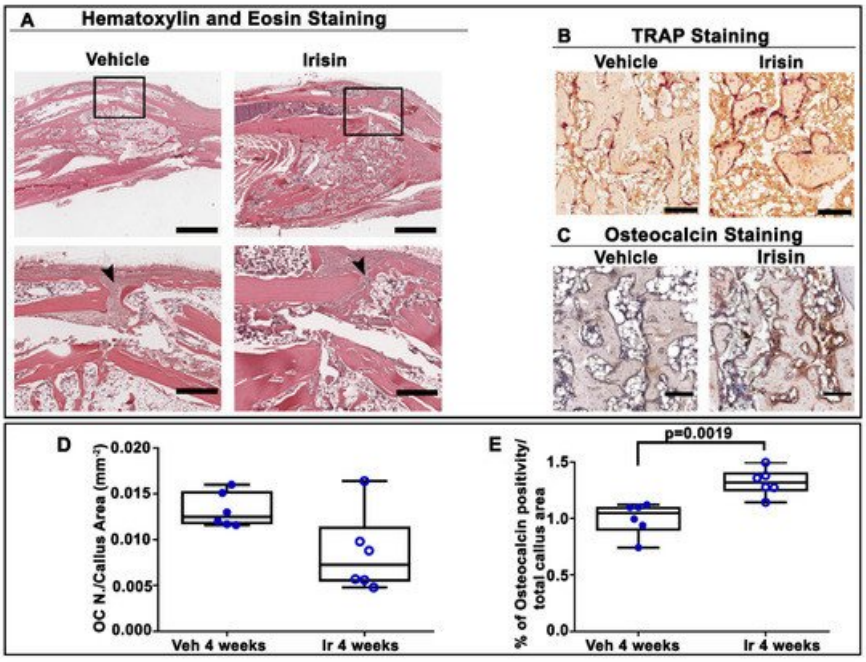

Figure 4. (**A**) Representative hematoxylin and eosin staining images on callus sections from vehicle- and irisin-treated mice at 28 days post-fracture (scale bar: 0.8 mm). The black squares indicate the area of higher magnification (scale bar: 60 Âµm). Arrowheads indicate the fibrous tissue. (**B**) Representative Trap staining images of callus sections from vehicle- and irisin-treated mice at 28 days post-fracture (scale bar: 30 Âµm). (**C**) Representative images of osteocalcin immunostaining in callus sections from vehicle- and irisin-treated mice at 28 days post-fracture (scale bar: 30 Âµm). (**D**) Quantification of OC N./CA in sections from vehicle- (n = 6) and irisin-treated mice (n = 6) at 28 days post-fracture. (**E**) Quantification of the percentage of osteocalcin-positive cells (osteocalcin^{+} cell, %) out of all cells of the callus from vehicle-treated mice (n = 6) and irisin-treated mice (n = 6) at 28 days post-fracture. Data are presented as dot-plots with medians, from maximum to minimum, with all data points shown. The MannâWhitney test was used to compare groups.

5. Conclusion

Systemic administration of intermittent low doses of irisin accelerates bone fracture healing in mice by promoting bone formation and mineralization. The transcription factor and matrix component expression analysis, histomorphometry and microCT data together demonstrate that irisin during fracture repair stimulates osteogenesis to produce more bone tissue that can stabilize the fracture more rapidly without altering the normal process of bone remodeling. Nevertheless, this study lays the basis for the use of recombinant irisin in fracture repair by providing a complementary analysis of tibial callus tissue following systemic irisin administration. Most importantly, we have added new data that increase our understanding of the processes that regulate and promote the conversion of cartilage to bone during fracture repair. Speculatively, our results may also provide a possible explanation for why bone fractures heal faster when muscle flaps are present at the fracture site: it could be irisin, produced by the muscle cells, that mediates this effect.

References

1. Ekegren, C.L.; Edwards, E.R.; de Steiger, R.; Gabbe, B.J. Incidence, Costs and Predictors of Non-Union, Delayed Union and Mal-Union Following Long Bone Fracture. Int. J. Environ. Res. Public

Health 2018, 15, 2845.

2. Svedbom, A.; Hernlund, E.; IvergÃ¥rd, M.; Compston, J.; Cooper, C.; Stenmark, J.; McCloskey, E.V.; JÃ¶nsson, B.; Kanis, J.A. Osteoporosis in the European Union: A compendium of country-specific reports. Arch. Osteoporos. 2013, 8, 137.
3. MÃ¼ller, F.; Galler, M.; Zellner, M.; BÃ¤uml, C.; FÃ¼chtmeier, B. Total hip arthroplasty after failed osteosynthesis of proximal femoral fractures: Revision and mortality of 80 patients. J. Orthop. Surg. 2017, 25, 2309499017717869.
4. Morice, A.; Ducellier, F.; Bizot, P. Total hip arthroplasty after failed fixation of a proximal femur fracture: Analysis of 59 cases of intra- and extra-capsular fractures. Orthop. Traumatol. Surg. Res. OTSR 2018, 104, 681â686.
5. Hak, D.J. The biology of fracture healing in osteoporosis and in the presence of anti-osteoporotic drugs. Injury 2018, 49, 1461â1465.
6. Bahney, C.S.; Zondervan, R.L.; Allison, P.; Theologis, A.; Ashley, J.W.; Ahn, J.; Miclau, T.; Marcucio, R.S.; Hankenson, K.D. Cellular biology of fracture healing. J. Orthop.Res. Off. Publ. Orthop. Res. Soc. 2019, 37, 35â50.
7. Wong, S.A.; Rivera, K.O.; Miclau, T., 3rd; Alsberg, E.; Marcucio, R.S.; Bahney, C.S. Microenvironmental Regulation of Chondrocyte Plasticity in Endochondral Repair-A New Frontier for Developmental Engineering. Front. Bioeng. Biotechnol. 2018, 6, 58.
8. Charlier, E.; Deroyer, C.; Ciregia, F.; Malaise, O.; Neuville, S.; Plener, Z.; Malaise, M.; de Seny, D. Chondrocyte dedifferentiation and osteoarthritis (OA). Biochem. Pharmacol. 2019, 165, 49â65.
9. Gerstenfeld, L.C.; Cullinane, D.M.; Barnes, G.L.; Graves, D.T.; Einhorn, T.A. Fracture healing as a post-natal developmental process: Molecular, spatial, and temporal aspects of its regulation. J. Cell. Biochem. 2003, 88, 873â884.
10. Kostenuik, P.; Mirza, F.M. Fracture healing physiology and the quest for therapies for delayed healing and nonunion. J. Orthop. Res. Off. Publ. Orthop. Res. Soc. 2017, 35, 213â223.
11. Liu, R.; Schindeler, A.; Little, D.G. The potential role of muscle in bone repair. J. Musculoskelet. Neuronal Interact. 2010, 10, 71â76.
12. Colaianni, G.; Storlino, G.; Sanesi, L.; Colucci, S.; Grano, M. Myokines and Osteokines in the Pathogenesis of Muscle and Bone Diseases. Curr. Osteoporos. Rep. 2020, 18, 401â407.
13. Buccoliero, C.; Oranger, A.; Colaianni, G.; Pignataro, P.; Zerlotin, R.; Lovero, R.; Errede, M.; Grano, M. The effect of Irisin on bone cells in vivo and in vitro. Biochem. Soc. Trans. 2021, 49, 477â484.
14. Pignataro, P.; Dicarlo, M.; Zerlotin, R.; Zecca, C.; Dellâ²Abate, M.T.; Buccoliero, C.; Logroscino, G.; Colucci, S.; Grano, M. FNDC5/Irisin System in Neuroinflammation and Neurodegenerative Diseases: Update and Novel Perspective. Int. J. Mol. Sci. 2021, 22, 1605.
15. Colaianni, G.; Cuscito, C.; Mongelli, T.; Pignataro, P.; Buccoliero, C.; Liu, P.; Lu, P.; Sartini, L.; Di Comite, M.; Mori, G.; et al. The myokine irisin increases cortical bone mass. Proc. Natl Acad. Sci. USA 2015, 112, 12157â12162.
16. Colaianni, G.; Mongelli, T.; Cuscito, C.; Pignataro, P.; Lippo, L.; Spiro, G.; Notarnicola, A.; Severi, I.; Passeri, G.; Mori, G.; et al. Irisin prevents and restores bone loss and muscle atrophy in hind-limb suspended mice. Sci. Rep. 2017, 7, 2811.
17. Colaianni, G.; Cuscito, C.; Mongelli, T.; Oranger, A.; Mori, G.; Brunetti, G.; Colucci, S.; Cinti, S.; Grano, M. Irisin enhances osteoblast differentiation in vitro. Int. J. Endocrinol. 2014, 2014, 902186.
18. Storlino, G.; Colaianni, G.; Sanesi, L.; Lippo, L.; Brunetti, G.; Errede, M.; Colucci, S.; Passeri, G.; Grano, M. Irisin Prevents Disuse-Induced Osteocyte Apoptosis. J. Bone Miner.Res. Off. J. Am. Soc. Bone Mineral. Res. 2020, 35, 766â775.

19. Kim, H.; Wrann, C.D.; Jedrychowski, M.; Vidoni, S.; Kitase, Y.; Nagano, K.; Zhou, C.; Chou, J.; Parkman, V.A.; Novick, S.J.; et al. Irisin Mediates Effects on Bone and Fat via Î±V Integrin Receptors. Cell 2018, 175, 1756â1768.e1717.
20. Estell, E.G.; Le, P.T.; Vegting, Y.; Kim, H.; Wrann, C.; Bouxsein, M.L.; Nagano, K.; Baron, R.; Spiegelman, B.M.; Rosen, C.J. Irisin directly stimulates osteoclastogenesis and bone resorption in vitro and in vivo. eLife 2020, 9, e58172.
21. Maak, S.; Norheim, F.; Drevon, C.A.; Erickson, H.P. Progress and Challenges in the Biology of FNDC5 and Irisin. Endocr. Rev. 2021, 42, 436â456.
22. Jedrychowski, M.P.; Wrann, C.D.; Paulo, J.A.; Gerber, K.K.; Szpyt, J.; Robinson, M.M.; Nair, K.S.; Gygi, S.P.; Spiegelman, B.M. Detection and Quantitation of Circulating Human Irisin by Tandem Mass Spectrometry. Cell Metab. 2015, 22, 734â740.
23. Ruan, Q.; Zhang, L.; Ruan, J.; Zhang, X.; Chen, J.; Ma, C.; Yu, Z. Detection and quantitation of irisin in human cerebrospinal fluid by tandem mass spectrometry. Peptides 2018, 103, 60â64.
24. Albrecht, E.; Schering, L.; Buck, F.; Vlach, K.; Schober, H.C.; Drevon, C.A.; Maak, S. Irisin: Still chasing shadows. Mol. Metab. 2020, 34, 124â135.
25. Anastasilakis, A.D.; Polyzos, S.A.; Makras, P.; Gkiomisi, A.; Bisbinas, I.; Katsarou, A.; Filippaios, A.; Mantzoros, C.S. Circulating irisin is associated with osteoporotic fractures in postmenopausal women with low bone mass but is not affected by either teriparatide or denosumab treatment for 3 months. Osteoporos. Int. 2014, 25, 1633â1642.
26. Palermo, A.; Strollo, R.; Maddaloni, E.; Tuccinardi, D.; Dâ²Onofrio, L.; Briganti, S.I.; Defeudis, G.; De Pascalis, M.; Lazzaro, M.C.; Colleluori, G.; et al. Irisin is associated with osteoporotic fractures independently of bone mineral density, body composition or daily physical activity. Clin. Endocrinol. 2015, 82, 615â619.
27. Faienza, M.F.; Brunetti, G.; Sanesi, L.; Colaianni, G.; Celi, M.; Piacente, L.; Dâ²Amato, G.; Schipani, E.; Colucci, S.; Grano, M. High irisin levels are associated with better glycemic control and bone health in children with Type 1 diabetes. Diabetes Res. Clin. Pract. 2018, 141, 10â17.
28. Colaianni, G.; Faienza, M.F.; Sanesi, L.; Brunetti, G.; Pignataro, P.; Lippo, L.; Bortolotti, S.; Storlino, G.; Piacente, L.; Dâ²Amato, G.; et al. Irisin serum levels are positively correlated with bone mineral status in a population of healthy children. Pediatric Res. 2019, 85, 484â488.
29. Colaianni, G.; Errede, M.; Sanesi, L.; Notarnicola, A.; Celi, M.; Zerlotin, R.; Storlino, G.; Pignataro, P.; Oranger, A.; Pesce, V.; et al. Irisin Correlates Positively With BMD in a Cohort of Older Adult Patients and Downregulates the Senescent Marker p21 in Osteoblasts. J. Bone Miner. Res. Off. J. Am. Soc. Bone Mineral. Res. 2021, 36, 305â314.
30. Singhal, V.; Lawson, E.A.; Ackerman, K.E.; Fazeli, P.K.; Clarke, H.; Lee, H.; Eddy, K.; Marengi, D.A.; Derrico, N.P.; Bouxsein, M.L.; et al. Irisin levels are lower in young amenorrheic athletes compared with eumenorrheic athletes and non-athletes and are associated with bone density and strength estimates. PLoS ONE 2014, 9, e100218.
31. Yan, J.; Liu, H.J.; Guo, W.C.; Yang, J. Low serum concentrations of Irisin are associated with increased risk of hip fracture in Chinese older women. Jt. Bone Spine 2018, 85, 353â358.
32. VadalÃ , G.; Di Giacomo, G.; Ambrosio, L.; Cannata, F.; Cicione, C.; Papalia, R.; Denaro, V. Irisin Recovers Osteoarthritic Chondrocytes In Vitro. Cells 2020, 9, 1478.
33. Wang, F.S.; Kuo, C.W.; Ko, J.Y.; Chen, Y.S.; Wang, S.Y.; Ke, H.J.; Kuo, P.C.; Lee, C.H.; Wu, J.C.; Lu, W.B.; et al. Irisin Mitigates Oxidative Stress, Chondrocyte Dysfunction and Osteoarthritis Development through Regulating Mitochondrial Integrity and Autophagy. Antioxidants 2020, 9, 810.